AMERICAN JOURNAL OF PHYSIOLOGY
HEART AND CIRCULATORY PHYSIOLOGY

Am J Physiol Heart Circ Physiol 329: H1017–H1030, 2025.
First published September 12, 2025; doi:10.1152/ajpheart.00194.2025

RESEARCH ARTICLE

Stress, Exercise and Cardiovascular Disease

Wave intensity analysis with exercise identifies impairments in pulmonary hypertension

Christopher G. Lechuga,[1]* Farhan Raza,[2]* Mitchel J. Colebank,[1,3] Claudia E. Korcarz,[2] Jens C. Eickhoff,[4] and Naomi C. Chesler[1]

[1]*Edwards Lifesciences Foundation Cardiovascular Innovation and Research Center (CIRC) and Department of Biomedical Engineering, University of California, Irvine, California, United States;* [2]*Department of Medicine, Cardiovascular Division, University of Wisconsin–Madison, Madison, Wisconsin, United States;* [3]*Department of Mathematics, University of South Carolina, Columbia, South Carolina, United States; and* [4]*Department of Biostatistics and Medical Informatics, University of Wisconsin–Madison, Madison, Wisconsin, United States*

Abstract

Wave intensity analysis provides a novel approach to understanding the dynamic interactions between the right ventricle and pulmonary vasculature, particularly in pulmonary hypertension, a condition characterized by elevated pulmonary arterial pressures and vascular remodeling. This prospective study used wave intensity analysis to evaluate right ventricular and pulmonary vascular mechanics in 22 participants with pulmonary hypertension (including precapillary, isolated postcapillary, and combined pre/postcapillary pulmonary hypertension), and three without pulmonary hypertension. Forward and backward compression and decompression waves were quantified at rest and during incremental exercise (25, 50, and 75 W). Relationships between metrics of wave intensity analysis, hemodynamics, right ventricular function, and oxygen consumption were analyzed using linear mixed-effects modeling. Wave intensity patterns highlighting vessel-specific pulmonary vascular and right ventricular pathobiology were observed in different phenotypes. Precapillary pulmonary hypertension exhibited highest forward compression waves, which correlated with right ventricular contractility ($P < 0.01$). Backward compression waves correlated strongly with characteristic impedance ($P = 0.002$) in combined pre/postcapillary pulmonary hypertension and inversely with pulmonary arterial compliance ($P = 0.003$) in precapillary pulmonary hypertension. The ratio of backward to forward compression (systolic) waves decreased in isolated postcapillary pulmonary hypertension during exercise ($P < 0.001$), suggesting right ventricular reserve capacity that improves vascular-ventricular coupling. Wave intensity metrics demonstrated strong correlations with oxygen consumption in participants without pulmonary hypertension, indicating sensitivity to exercise-induced changes in cardiopulmonary status. Wave intensity analysis with exercise suggests vessel-specific pulmonary vascular and right ventricular characteristics unique to pulmonary hypertension phenotypes. These findings highlight wave intensity analysis as a promising tool for advancing understanding of cardiopulmonary pathobiology in pulmonary hypertension.

NEW & NOTEWORTHY Wave intensity analysis (WIA) during exercise reveals distinct ventricle-/vessel-specific impairments across PH phenotypes. Cpc-PH exhibited highest forward and backward compression waves, reflecting elevated RV energy expenditure and pulmonary vascular stiffness, respectively. Precapillary PH demonstrated higher forward and backward decompression waves, suggesting differences in RV and pulmonary vascular mechanics. The compression reflection index decreased in Ipc-PH with exercise, indicating RV reserve capacity. These findings highlight WIA's potential for phenotyping PH and advancing cardiopulmonary pathophysiology assessment.

invasive cardiopulmonary exercise testing; pulmonary hypertension; right ventricular function; ventricular-vascular coupling; wave intensity analysis

INTRODUCTION

Pulmonary hypertension (PH) is a challenging, multifactorial condition characterized by increased pressure in the pulmonary vasculature (1), leading to right ventricular (RV) dysfunction (2) and significant mortality (3). Despite advances in diagnostic and therapeutic approaches, PH continues to present clinical dilemmas due to its heterogeneous

*C. G. Lechuga and F. Raza contributed equally to this work.
Correspondence: N. C. Chesler (nchesler@uci.edu).
Submitted 17 March 2025 / Revised 15 April 2025 / Accepted 3 September 2025

biological nature and the limitations of current diagnostic techniques (2, 4, 5). Conventional assessments focus on static measures obtained at rest, which do not fully capture the dynamic nature of both ventricular and vascular functions, masking early disease manifestations (6, 7). As a consequence, there is an average delay of 3 years between symptom onset and accurate diagnosis and treatment initiation (8, 9), underscoring the critical need for more sensitive and comprehensive diagnostic tools that can capture the complex pathobiology of pulmonary vascular disease.

Incorporating the pulsatile component of pulmonary hemodynamics represents one solution to this diagnostic challenge (7). Although traditional assessments are based on mean pulmonary artery pressure (mPAP), pulmonary arterial wedge pressure (PAWP), and pulmonary vascular resistance (PVR) at rest (i.e., static or steady-state metrics) (10), the pulsatility of blood flow and dynamic interactions between pressure and flow waves, especially under stress (e.g., exercise), could provide valuable insights into both RV and pulmonary vascular pathophysiology in PH (9). Recently, there has been growing interest in wave intensity analysis (WIA) as a novel approach to assess pulsatile pulmonary hemodynamics (11–13).

WIA quantifies the propagation and interaction of blood pressure and flow waves (13–15). The four most commonly reported metrics of WIA relate to ventricle- and vessel-specific mechanics and are largely cardiac-cycle specific: the forward compression waves (FCWs), backward compression waves (BCWs), forward decompression waves (FDWs), and backward decompression waves (BDWs). Figure 1 provides a conceptual overview of the wave types, their timing, and physiological interpretation. In systemic and pulmonary circulations, FCWs are established as markers of ventricular force generation during early systole, and BCWs are associated with wave reflections from proximal arteries, often influenced by proximal artery stiffness or impedance mismatch (11, 13–17). These two types of waves typically occur during systole and are thus considered systolic waves. Although the interpretations of the decompression waves (FDWs and BDWs) are less consistent than those of the compression waves, FDWs are generally considered to reflect ventricular relaxation, and BDWs are suggested to reflect distal vascular properties, such as stiffness and/or compliance (14–17). FDWs and BDWs typically occur during diastole and are considered diastolic waves.

Together, these components reflect the complex interplay between RV function, RV-pulmonary artery (PA) coupling, and proximal and distal pulmonary vascular mechanics (13, 14, 18, 19), offering a deeper understanding of the cardiopulmonary system, which is crucial for diagnosing and understanding the severity and progression of PH (11–13, 19, 20). In addition to characterizing ventricular and pulmonary vascular properties in-depth, the clinical and physiological relevance of WIA metrics can be assessed via their relationships with oxygen consumption ($\dot{V}O_2$). $\dot{V}O_2$ reflects the body's ability to uptake, deliver, and extract oxygen efficiently across multiple physiological systems, making it a comprehensive marker of functional capacity and cardiovascular health (21, 22).

The present study quantifies key WIA metrics from rest to exercise conditions in PH phenotypes, including precapillary PH, isolated postcapillary PH (Ipc-PH), and combined pre- and postcapillary PH (Cpc-PH). Our broader hypothesis is that the different components of WIA are ventricle- and pulmonary vessel-specific and their changes from rest to exercise are specific to PH phenotypes. Using precapillary PH and no PH subtypes as comparison, we focus on postcapillary PH subtypes (Ipc-PH and Cpc-PH) due to limited treatments and poor understanding of pathobiology in these PH subtypes. Our specific hypothesis in postcapillary PH is that as the disease progresses from Ipc-PH to Cpc-PH, WIA metrics capture: *1*) increased RV energy expenditure and contraction (higher FCW), *2*) proximal PA remodeling and stiffness (higher BCW), *3*) poor RV relaxation despite increased RV afterload (generating lower intensity FDW), and *4*) poor flow acceleration in diastole due to remodeling and stiffness of distal pulmonary vasculature [generating higher BDW, in relation to FDW

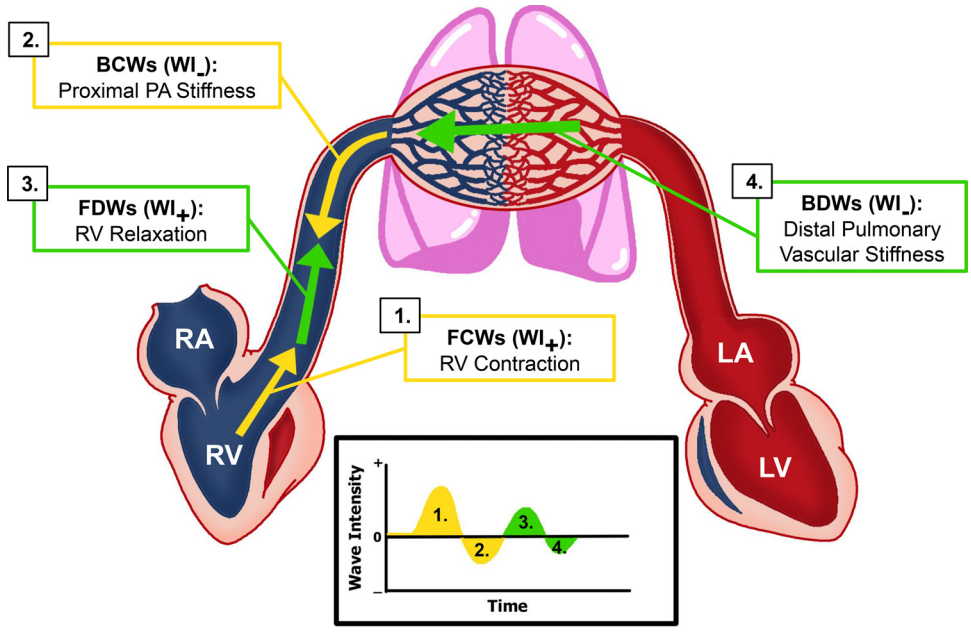

Figure 1. Conceptual framework of pulmonary vascular wave mechanics. This figure provides an abstract overview of the four components of wave intensity analysis (WIA): *1*) forward compression waves, *2*) backward compression waves, *3*) forward decompression waves, and *4*) backward decompression waves (FCWs, BCWs, FDWs, BDWs, respectively) and their origins within the cardiopulmonary system.

intensity, a phenomenon captured by increased diastolic (decompression) reflection index = BDW/FDW]. By defining these intricate RV- and pulmonary vessel-specific WIA components, we seek to advance our understanding of PH pathophysiology and explore the potential of WIA as a complementary diagnostic tool in managing PH.

MATERIALS AND METHODS

All participants provided informed consent in agreement with guidelines approved by the UW-Madison institutional review board (IRB ID: 2019-1184). The study complied with the guidelines of the Declaration of Helsinki and was overseen by an independent safety and monitoring board.

Study Population

Twenty-seven adult participants (16 female, 11 male), referred for invasive cardiopulmonary exercise testing (iCPET) for New York Heart Association (NYHA) functional class II-III dyspnea evaluation, were enrolled in this multistep, rest-to-exercise-to-recovery study protocol. Inclusion criteria were as follows: dyspnea with New York Heart Association (NYHA) functional class II-III, evidence of PH on echocardiogram, and ability to participate in exercise testing. Exclusion criteria included: age >80 yr, body mass index > 40.0 Kg/m^2, NYHA I or IV, contraindications to MRI, active cardiac problems (angina or unstable arrhythmias), implanted pacemaker or defibrillator, left ventricular ejection fraction <50%, lung parenchymal disease requiring supplemental oxygen, end-stage renal disease or chronic kidney disease (creatinine >2.0 mg/dL), any acute illness, or recent hospitalization within the prior 3 mo. PH phenotype was diagnosed in participants based on hemodynamic measurements (mPAP, PAWP, and PVR) obtained via right heart catheterization (RHC) at rest, according to 2022 ESC/ERS guidelines (10). Of the 27 participants enrolled, two had uninterpretable data due to motion artifact during iCPET and were excluded. The remaining 25 enrolled participants were then categorized based on disease location as: precapillary PH [including pulmonary arterial hypertension (PAH, $n = 3$), chronic thromboembolic PH (CTEPH, $n = 2$)], Ipc-PH ($n = 12$), Cpc-PH ($n = 5$), and those without PH (No PH, $n = 3$) (10). Note that the No PH group was referred for iCPET based on subjective dyspnea. Given their relatively normal cardiopulmonary hemodynamics, their dyspnea was likely related to other comorbidities (obesity or cardiometabolic conditions, e.g., diabetes, hypertension) and/or musculoskeletal deconditioning. In addition, according to the World Health Organization (WHO) classification, precapillary PH included PAH (WHO group 1) and CTEPH (WHO group 4), whereas Ipc-PH and Cpc-PH fall under WHO group 2 (PH due to left heart disease) (10). The Ipc-PH and Cpc-PH participants had PH due to heart failure with preserved ejection fraction (PH-HFpEF). A subset of data from 4 of the 25 participants (1 No PH, 1 CTEPH, 1 PAH, and 1 PH-HFpEF) was previously reported (9).

iCPET and Echocardiogram

All participants underwent iCPET in the semi-recumbent position using a cycle ergometer as the mode of exercise (23, 24). This included simultaneous RHC at rest and exercise (data acquired every 25 W), radial arterial line monitoring, and gas exchange data acquisition in addition to simultaneous pulsed-wave Doppler (PWD) echocardiography of the right ventricular outflow tract (RVOT) to take the spatially averaged velocity (U), as previously described (details in Supplemental Data) (9, 25).

Pulse wave doppler (PWD) echocardiogram of right ventricular outflow tract (RVOT) for flow and velocity signal was acquired simultaneously as pulmonary artery pressure at each stage (rest, every 25 W of exercise, 5-min into recovery). RVOT PWD data were only included in analyses if signal quality was adequate, and 3–5 beats were available at each stage to take the average of the velocity over the RVOT area (U). Exercise datapoints were excluded if echocardiographic windows were limited (poor quality RVOT signal or inaccurate sample volume).

For pressure signal, a 4-Fr high-fidelity Millar catheter was used for pulmonary artery pressure (PAP) measurement, and a 7 Fr fluid-filled was used for RV pressure (RVP). Baseline invasive hemodynamic measurements (pressures and direct Fick cardiac output) and echocardiographic (RVOT PWD) recordings were obtained at rest. Simultaneous recordings of PAP and RVOT PWD signals were acquired for WIA. Subsequently, participants engaged in exercise, beginning with 2 min of unloaded peddling, followed by an incremental ramp protocol at a rate of 10 W/min (maintaining a constant cycling cadence of 60 rpm throughout). At every 25 W, the incremental protocol was held at that stage, and simultaneous PAP (via Millar catheter) and RVOT PWD were acquired. After peak symptom-limited exercise, simultaneous PAP and echocardiographic doppler data were acquired 5-min into recovery.

At each exercise stage (e.g., 25 W, 50 W, etc.), participants exercised for 4–5 min, and data was acquired only after first 2 min when a steady and consistent heart rate was achieved for that exercise stage. This reduced noise and breathing artifacts, and reduced any variability of heart rates, resulting in a noise-free ensemble-averaged representative waveform. Simultaneous recordings of RVOT velocity U and PAP were aligned in time for wave intensity analysis. $\dot{V}O_2$, or oxygen consumption, was measured continuously during the iCPET using a metabolic cart (Metabolic Ultima CardiO2; MedGraphics). A second stage of rest-exercise-recovery was performed to acquire right ventricular (RV) pressure volume loops, and metrics were constructed and calculated, respectively, as previously described (9). All participants exercised to maximal volitional effort.

$\dot{V}O_2$ acquisition and measurement.

Participants breathed through a mouthpiece connected to the metabolic cart, which measured the volume and concentration of oxygen (O_2) and carbon dioxide (CO_2) in the inhaled and exhaled air. $\dot{V}O_2$ was calculated using the breath-by-breath method, accounting for the differences in O_2 and CO_2 concentrations between inspiration and expiration. The highest $\dot{V}O_2$ value achieved during exercise was recorded as peak $\dot{V}O_2$, which reflects the participant's maximal aerobic capacity. Data were collected at rest, during exercise, and at recovery.

Relationships between WIA components (FCWs, BCWs, FDWs, and BDWs) and $\dot{V}O_2$ for all PH phenotypes were investigated through linear regression models, where logarithmic

transformations of both WIA components and $\dot{V}O_2$ were performed to account for differences in magnitude, and the best-fit values of the phenotype-specific slopes were compared using the extra sum-of-squares F test.

Analysis of Wave Speed, Wave Intensity, and Wave Separation

From continuously obtained, time-dependent, PAP and U waveforms, 4–15 PAP waveforms and 2–3 U waveforms were selected that were free from motion artifacts and ensemble-averaged to create representative single-beat waveforms. The early systolic segment of pressure was then aligned with the early systolic segment of velocity, creating PU loops for wave intensity analyses. Wave speed c (in m/s) was calculated using:

$$c = \frac{1}{\rho}\sqrt{\frac{\sum dP^2}{\sum dU^2}} \quad (1)$$

where ρ is the density of blood (assumed equal to 1,040 kg/m^3), dP is the point-to-point change in the single-beat PAP waveform over an interval dt (in mmHg), and dU is the change in the single-beat velocity waveform over the same interval dt (in m/s) (14). Then waves were separated into their forward and backward components via the following equation:

$$WI_{\pm} = \left(\frac{dP \times CCD}{dt} \pm \frac{dU \times CCD}{dt}\right)^2 / (4\rho c) \quad (2)$$

where dP is the change in pressure, dU is the change in velocity, dt is the time interval, and CCD is the cardiac cycle duration (inverse of heart rate) (14). WI_+ indicates wave propagation in the forward direction in the PA (away from the RV), and WI_- indicates wave propagation in the backward direction in the PA (toward the RV; see Fig. 1) (13, 14). The waves were further defined as compression (i.e., increasing pressure) or decompression (i.e., decreasing pressure) components (13, 14). FCWs were characterized by an increase in both pressure and velocity, whereas BCWs were characterized by an increase in pressure but a decrease in velocity (13, 14). FDWs were characterized by a decrease in both pressure and velocity, whereas BDWs were characterized by a decrease in pressure but an increase in velocity (13, 14).

Statistical Analysis

All hemodynamic data are presented as means ± SD. Wave intensity analyses were performed with MATLAB (The MathWorks, Inc., Natick, MA, version R2020b). An analysis of variance (ANOVA) was used to compare means of clinical and basic hemodynamic parameters among the precapillary PH, Ipc-PH, Cpc-PH, and No PH phenotypes. To ensure consistency in scale, we log-transformed both WIA and $\dot{V}O_2$ values before correlative assessment. Post hoc comparisons were conducted using the Tukey–Kramer test to adjust for multiple comparisons. An unpaired t test was used to compare means of indices between rest and initial exercise within each phenotype. A linear mixed effects modeling approach with participant-specific random effects and a compound symmetry structure to account for repeated measures under various exposure conditions were used to conduct comparisons of each outcome measure between PH phenotypes at each exercise stage and disease-specific correlation analyses. The modeling included phenotype, stage, and phenotype-stage interaction effects as predictor variables. A sliced contrast was used to compare phenotypes at each stage. For disease-specific correlation analysis, an autoregressive correlation structure of order one was used. This model is used in time-series analysis to account for temporal dependencies, where consecutive observations are expected to be more correlated than observations further apart in time. Hence, it accounts for repeated measures between stages within the same participants. Statistical analysis and correlation plots were conducted using SAS software (SAS Institute, Cary NC, version 9.4) and Prism (GraphPad Software, San Diego, CA, version 9.2.0). All reported P values are two-sided, and P value < 0.05 was used to determine statistical significance.

RESULTS

Clinical, echocardiography, and cardiac MRI characteristics are presented in Table 1. The iCPET data, including workload, gas exchange, metrics of steady-state, and pulsatile hemodynamics, are provided in Table 2. The number of participants able to achieve each exercise workload are also indicated in Table 2. Peak workload was defined as the maximum workload achieved by a participant during the incremental exercise test, typically determined by symptom limitation or clinical assessment of intolerance. The results of the linear mixed-effects modeling approach comparing WIA metrics with related standard clinical RV and pulmonary vascular function metrics are presented in Table 3, and key findings across PH phenotypes are summarized in Table 4.

WIA in PH Phenotypes

At rest, Cpc-PH had the highest forward compression waves (FCWs) (Fig. 2*A*), suggesting greater RV systolic force generation. During initial exercise (25 W), FCWs increased the most in Cpc-PH, with smaller increases in precapillary PH and Ipc-PH. The smaller increase in FCWs in the Ipc-PH phenotype with exercise, which was significant at maximum exercise (100 W) ($P < 0.05$, Fig. 2*A*), suggests less RV force generation. FCWs in No PH were consistently lower across all exercise stages, due to lower pressures and/or lower velocities and consequently lower demand for RV force (Table 2). At recovery, FCWs remained elevated in the precapillary PH phenotype ($P < 0.01$, Fig. 2*A*).

At rest, backward compression waves (BCWs) were also highest in Cpc-PH (Fig. 2*B*), suggesting a prominent reflection arriving to the RV from a stiffened pulmonary arterial network (see Fig. 1). During exercise, BCWs tended to increase in all phenotypes except Ipc-PH. No differences between BCWs in Ipc-PH and precapillary PH were evident. At recovery, BCWs remained elevated in the precapillary PH phenotype compared with the Ipc-PH and No PH phenotypes ($P < 0.01$, Fig. 2*B*). BCWs also remained elevated in the Cpc-PH phenotype, suggesting an impaired return to low RV afterload and poor recovery postexercise.

Forward decompression waves (FDWs) were highest in precapillary PH at rest and exercise (Fig. 2*C*). With exercise stages, FDWs in precapillary PH were nearly double those in Ipc-PH ($P < 0.05$, Fig. 2*C*), which suggests better RV

Table 1. *Clinical, echocardiography, and cardiac MRI characteristics*

PH Phenotype	Precapillary PH (n = 5)†	Ipc-PH (n = 12)	Cpc-PH (n = 5)	No PH (n = 3)
Age, yr	60 ± 17	64 ± 8	76 ± 4	66 ± 4
Female sex, *n* (%)	4 (80)	5 (42)	5 (100)	2 (67)
BMI, kg/m^2	29.9 ± 6.2	33.8 ± 6.0	31.9 ± 11.2	32.8 ± 5.2
6MWD, m	316 ± 73	286 ± 90	198 ± 55	302 ± 134
KCCQ score	67 ± 15	60 ± 20	61 ± 15	79 ± 14
NYHA class (median)	2	2	3	2
WHO group				
I	3			
II		12	5	
IV	2			
Medications, *n*				
Diuretic	3	5	4	1
MRA	2	6	3	0
Anticoagulant	2	6	3	0
Comorbidities, *n*				
Hypertension	3	9	3	1
Diabetes	2	6	3	1
CAD	2	4	2	0
Sleep apnea	2	8	3	2
Atrial fibrillation	0	4	2	1
Scleroderma	2	3	2	2
PE	2	3	0	2
Laboratory work				
Hemoglobin, g/dL	13.3 ± 1.3	13.5 ± 2.7	13.6 ± 0.5	13.8 ± 1.8
Creatinine, mg/dL	1.1 ± 0.4	1.1 ± 0.3	1.0 ± 0.3	0.8 ± 0.1
BNP, pg/mL	148 ± 120	81 ± 88	180 ± 90	30 ± 18
Echocardiogram				
LVEF (%)	61 ± 4	63 ± 3	63 ± 3	65 ± 1
RV:LV	1.0 ± 0.1	0.9 ± 0.1	0.8 ± 0.2	0.9 ± 0.1
TAPSE, cm	2.0 ± 0.4	2.3 ± 0.4	1.7 ± 0.3	2.3 ± 0.1
Ecc. index	1.0 ± 0.1	1.0 ± 0.1	1.1 ± 0.1	0.9 ± 0.1
LAVI, mL/m^2	26 ± 6	28 ± 9	33 ± 4	25 ± 7
Average E/E′	9 ± 5	10 ± 3	12 ± 3	7 ± 1
RVOT acc. time, ms	93 ± 7	112 ± 12	77 ± 6	127 ± 33
RVOT notch, *n*	2	0	2	0
Cardiac MRI				
RVEF, %	52 ± 12	54 ± 11	47 ± 10	55 ± 14
RVEDVi, mL/m^2	67 ± 22	70 ± 18	68 ± 18	69 ± 11
RVESVi, mL/m^2	35 ± 20	33 ± 15	39 ± 14	33 ± 15
LVEF, %	65 ± 3	60 ± 10	63 ± 2	61 ± 4
LVEDVi, mL/m^2	53 ± 12	66 ± 13	65 ± 3	68 ± 12
LVESVi, mL/m^2	19 ± 5	27 ± 10	20 ± 6	23 ± 10

Values are means ± SD. 6MWD, six-minute walk distance; BMI, body mass index; BNP, B-type natriuretic peptide; CAD, coronary artery disease; CMR, cardiac magnetic resonance imaging; Cpc-PH, combined pre- and postcapillary pulmonary hypertension; E/E′, ratio of early diastolic velocity of mitral inflow to early diastolic tissue Doppler velocity of the lateral mitral annulus; Ecc. index, eccentricity index; Ipc-PH, isolated postcapillary pulmonary hypertension; KCCQ, Kansas City Cardiomyopathy Questionnaire; LAVI, left atrial volume index; LVEDVi, left ventricular end-diastolic volume index; LVEF, left ventricular ejection fraction; LVESVi, left ventricular end-systolic volume index; MRA, mineralocorticoid receptor antagonists; NYHA, New York Heart Association; PE, pulmonary embolism; PH, Pulmonary hypertension; RV, residual volume; RVEDVi, right ventricular end-diastolic volume index; RVEF, right ventricular ejection fraction; RVESVi, right ventricular end-systolic volume index; RV:LV, right ventricle-to-left ventricle diameter ratio; RVOT, right ventricular outflow tract; TAPSE, tricuspid annular plane systolic excursion; WHO, World Health Organization. †Precapillary PH participants were not taking PAH medications at the time of the study. These participants started PAH therapies afterward.

relaxation in precapillary PH. As with other elements of the WIA, FDWs at recovery remained elevated in the pre-capillary PH phenotype.

The backward decompression waves (BDWs) have been interpreted as a reflection of distal vascular properties during diastole in the coronary circulation (17), such as distal stiffness, as illustrated in Fig. 1. BDWs were highest in the precapillary PH during exercise despite similar values at rest (Fig. 2*D*).

Pulmonary Arterial Wave Speed in PH Phenotypes

Wave speed increases in smaller, stiffer arteries and decreases in larger, more compliant arteries (26). High pressures can either increase wave speed by increasing stiffness, decrease wave speed by increasing diameter, or cause no change due to a combination of these effects (26). Here, we found higher wave speeds in the Cpc-PH and precapillary PH phenotypes, and lower wave speeds in the Ipc-PH and No PH phenotypes with minimal changes as a function of exercise workload (Fig. 3).

Wave Reflection Indices in PH Phenotypes

To measure the relative amount of the energy of the ejection wave (forward wave) that is reflected back toward the RV (backward wave), we calculated the two reflection indices: the compression (systolic) reflection index (BCWs:FCWs) and the decompression (diastolic) reflection index (BDWs:FDWs) at rest and initial exercise for all phenotypes (Figs. 4 and 5). At rest, the compression reflection indices had high variability, and no differences between PH phenotypes were evident ($P = 0.06$) (Fig. 4). When comparing rest to 25 W exercise conditions, however, the compression reflection index significantly decreased in the Ipc-PH phenotype ($P < 0.001$) and did not change significantly in other phenotypes. The decompression reflection index also showed no differences between phenotypes at rest, nor were there differences within each phenotype from rest to initial exercise (25 W, Fig. 5).

WIA Components Correlate Differently with $\dot{V}O_2$

To define the clinical relevance of wave intensity metrics, we examined their correlation with oxygen consumption ($\dot{V}O_2$), a key indicator of efficient gas exchange and a recognized prognostic marker in PH (21). In the overall combined cohort ($n = 25$), there was a significant, weak positive correlation between FCWs and $\dot{V}O_2$ (Table 3; $r = 0.16$, 95% CI [0.02–0.31], $P = 0.02$). Correlations were not significant in individual phenotypes (Supplemental Fig. S1; see https://doi.org/10.5281/zenodo.16500282), but in the No PH phenotype, there was a stronger positive correlation between FCWs and $\dot{V}O_2$ than in the other phenotypes (Table 3; slope = 0.60, $r = 0.39$, 95% CI [−0.17 to 0.96]). Cpc-PH had the weakest correlation (slope = 0.31, $r = 0.10$, 95% CI [−0.61 to 0.81]). Interestingly, there was a highly significant and strong positive correlation between BCWs and $\dot{V}O_2$ in the No PH phenotype (slope = 0.80, $r = 0.92$, 95% CI [0.72–0.98], $P < 0.0001$), whereas in the combined cohort as well as other phenotypes, there were very weak or no correlations and no significance (Table 3).

In the overall combined cohort, there was a significant, weak positive correlation between FDWs and $\dot{V}O_2$ (Table 3;

Table 2. *Invasive CPET data including workload, gas exchange, and metrics of steady-state and pulsatile hemodynamics during exercise*

PH Phenotype	Precapillary PH ($n = 5$)	Ipc-PH ($n = 12$)	Cpc-PH ($n = 5$)	No PH ($n = 3$)
Peak workload, W	67 ± 35	76 ± 32	28 ± 8	72 ± 22
Peak $\dot{V}O_2$, mL/kg/min	12.0 ± 5.1	17.5 ± 5.1	9.8 ± 3.1	18.6 ± 4.0
Peak $\dot{V}O_2$, % predicted	54 ± 21	66 ± 16	49 ± 9	77 ± 8
$\dot{V}O_2$, mL/kg/min				
Rest	227 ± 62 (n = 5)	276 ± 50 ($n = 11$)	208 ± 37 ($n = 5$)	246 ± 52 ($n = 3$)
25 W	574 ± 107 ($n = 5$)	732 ± 194 ($n = 11$)	563 ± 123 ($n = 5$)	678 ± 144 ($n = 3$)
50 W	776 ± 152 ($n = 3$)	870 ± 204 ($n = 8$)		896 ± 194 ($n = 3$)
75 W	1,001 ± 178 ($n = 3$)	1,085 ± 192 ($n = 8$)		
100 W	1,052 ± 68 ($n = 2$)	1,353 ± 253 ($n = 5$)		
Recovery	351 ± 75 ($n = 5$)	418 ± 122 ($n = 8$)	310 ± 32 ($n = 5$)	324 ± 51 ($n = 3$)
Peak RER	1.03 ± 0.11	0.95 ± 0.11	0.89 ± 0.10	1.00 ± 0.20
$\dot{V}E/\dot{V}CO_2$ slope	41 ± 9	33 ± 8	39 ± 11	33 ± 7
OUES	1.11 ± 0.32	1.66 ± 0.48	1.17 ± 0.53	1.45 ± 0.47
Heart rate, beats/min				
Rest	71 ± 9	72 ± 9 ($n = 12$)	69 ± 11	87 ± 6
25 W	93 ± 10	93 ± 15 ($n = 12$)	99 ± 30	103 ± 6
50 W	109 ± 3	101 ± 17 ($n = 9$)		117 ± 8
75 W	122 ± 7	109 ± 16 ($n = 9$)		
100 W	134 ± 4	106 ± 7 ($n = 5$)		
Recovery	97 ± 14	80 ± 14 ($n = 8$)	82 ± 23	94 ± 11
CO, L/min				
Rest	4.7 ± 1.2	6.2 ± 1.4 ($n = 12$)	4.4 ± 1.5	6.1 ± 1.9
25 W	7.2 ± 2.0	9.0 ± 2.8 ($n = 12$)	6.2 ± 2.1	8.7 ± 1.7
50 W	8.5 ± 3.0	9.6 ± 2.0 ($n = 9$)		11.3 ± 1.9
75 W	9.8 ± 3.0	11.0 ± 2.0 ($n = 9$)		
100 W	8.5 ± 1.7	11.8 ± 2.2 ($n = 5$)		
Recovery	4.6 ± 1.4	8.4 ± 2.0 ($n = 8$)	5.8 ± 3.3	7.9 ± 2.1
mPAP, mmHg				
Rest	31 ± 8	26 ± 6 ($n = 12$)	42 ± 6	20 ± 2
25 W	45 ± 5	42 ± 9 ($n = 12$)	58 ± 12	28 ± 3
50 W	46 ± 5	44 ± 8 ($n = 9$)		31 ± 3
75 W	49 ± 6	46 ± 8 ($n = 9$)		
100 W	50 ± 7	49 ± 7 ($n = 5$)		
Recovery	25 ± 19	36 ± 8 ($n = 8$)	58 ± 7	24 ± 2
PAWP, mmHg				
Rest	13 ± 2	16 ± 4 ($n = 12$)	20 ± 3	10 ± 2
25 W	18 ± 3	25 ± 6 ($n = 12$)	31 ± 4	17 ± 1
50 W	21 ± 3	26 ± 4 ($n = 9$)		17 ± 1
75 W	22 ± 3	29 ± 4 ($n = 9$)		
100 W	21 ± 3	30 ± 5 ($n = 5$)		
Recovery	12 ± 8	22 ± 4 ($n = 8$)	30 ± 2	15 ± 2
PAC, mL/mmHg				
Rest	3.4 ± 1.3	5.4 ± 1.6 ($n = 12$)	1.7 ± 0.7	6.4 ± 3.2
25 W	2.6 ± 1.1	4.2 ± 1.3 ($n = 12$)	1.8 ± 1.3	7.9 ± 3.7
50 W	2.5 ± 0.8	3.8 ± 1.2 ($n = 9$)		6.1 ± 1.9
75 W	2.0 ± 0.5	3.7 ± 1.4 ($n = 9$)		
100 W	1.3 ± 0.0	3.0 ± 1.3 ($n = 5$)		
Recovery	3.2 ± 1.6	4.6 ± 2.1 ($n = 8$)	1.8 ± 1.4	6.8 ± 1.0
PVR, mmHg·min/L				
Rest	4.34 ± 2.06	1.73 ± 0.59 ($n = 12$)	5.74 ± 2.44	1.76 ± 0.39
25 W	4.15 ± 1.04	2.11 ± 0.73 ($n = 12$)	5.43 ± 2.21	1.43 ± 0.55
50 W	3.53 ± 0.97	2.06 ± 0.75 ($n = 9$)		1.36 ± 0.36
75 W	3.20 ± 0.73	1.83 ± 0.65 ($n = 9$)		
100 W	3.74 ± 0.12	1.98 ± 0.77 ($n = 5$)		
Recovery	4.48 ± 1.62	1.83 ± 0.50 ($n = 8$)	7.24 ± 5.01	1.30 ± 0.36
Z_C, mmHg·min/L				
Rest	0.70 ± 0.20	0.20 ± 0.12 ($n = 12$)	1.06 ± 0.27	0.34 ± 0.01
25 W	0.65 ± 0.29	0.47 ± 0.16 ($n = 12$)	1.43 ± 0.60	0.22 ± 0.03
50 W	0.70 ± 0.39	0.51 ± 0.24 ($n = 9$)		0.22 ± 0.07
75 W	0.67 ± 0.30	0.42 ± 0.16 ($n = 9$)		
100 W	0.64 ± 0.34	0.48 ± 0.18 ($n = 5$)		
Recovery	0.59 ± 0.17	0.30 ± 0.15 ($n = 8$)	1.12 ± 0.51	0.12 ± 0.13
E_{es}, mmHg/mL				
Rest	0.27 ± 0.09 ($n = 5$)	0.28 ± 0.12 ($n = 12$)	0.63 ± 0.57 ($n = 5$)	0.24 ± 0.06 ($n = 3$)
25 W	0.37 ± 0.08 ($n = 5$)	0.24 ± 0.10 ($n = 12$)	0.69 ± 0.57 ($n = 5$)	0.22 ± 0.03 ($n = 3$)
50 W	0.33 ± 0.08 ($n = 3$)	0.30 ± 0.11 ($n = 9$)		0.30 ± 0.04 ($n = 3$)

Continued

Table 2.— *Continued*

PH Phenotype	Precapillary PH ($n = 5$)	Ipc-PH ($n = 12$)	Cpc-PH ($n = 5$)	No PH ($n = 3$)
75 W	0.37 ± 0.20 ($n = 3$)	0.30 ± 0.13 ($n = 9$)		
100 W	0.64 ± 0.30 ($n = 2$)	0.37 ± 0.24 ($n = 5$)		
Recovery	0.30 ± 0.10 ($n = 5$)	0.37 ± 0.22 ($n = 8$)	0.66 ± 0.40 ($n = 5$)	0.28 ± 0.16 ($n = 3$)
E_a, mmHg/mL				
Rest	0.50 ± 0.20	0.26 ± 0.10	1.27 ± 1.44	0.23 ± 0.08
25 W	0.65 ± 0.30	0.41 ± 0.10	1.20 ± 0.68	0.24 ± 0.07
50 W	0.54 ± 0.06	0.44 ± 0.11		0.24 ± 0.02
75 W	0.72 ± 0.03	0.46 ± 0.12		
100 W	1.10 ± 0.36	0.60 ± 0.24		
Recovery	0.50 ± 0.26	0.26 ± 0.10	1.26 ± 1.08	0.23 ± 0.00
E_{es}/E_a				
Rest	0.58 ± 0.22	1.09 ± 0.33	0.58 ± 0.27	1.05 ± 0.10
25 W	0.61 ± 0.12	0.61 ± 0.22	0.52 ± 0.28	0.98 ± 0.26
50 W	0.62 ± 0.17	0.70 ± 0.24		1.26 ± 0.24
75 W	0.51 ± 0.28	0.66 ± 0.22		
100 W	0.56 ± 0.09	0.60 ± 0.23		
Recovery	0.63 ± 0.12	1.00 ± 0.42	0.59 ± 0.14	1.25 ± 0.72

Values are means ± SD. CO, cardiac output; Cpc-PH, combined pre and postcapillary pulmonary hypertension; CPET, cardiopulmonary exercise test; dPAP, diastolic pulmonary arterial pressure; Ipc-PH, isolated postcapillary pulmonary hypertension; mPAP, mean pulmonary arterial pressure; PAC, pulmonary arterial compliance; PAWP, pulmonary arterial wedge pressure; PH, pulmonary hypertension; PVR, pulmonary vascular resistance; RER, respiratory exchange ratio; $\dot{V}E/\dot{V}CO_2$, minute ventilation to carbon dioxide production ratio; $\dot{V}O_2$, oxygen consumption; Z_C, characteristic impedance.

$r = 0.20$, 95% CI [0.05–0.34], $P = 0.008$). In the Ipc-PH phenotype, there was a significant and weak, positive correlation between FDWs and $\dot{V}O_2$ (Table 3; slope = 0.54, $r = 0.25$, 95% CI [0.07–0.43], $P = 0.008$) and no correlation in the precapillary PH phenotype. Although none were significant, there were stronger positive correlations between BDWs and $\dot{V}O_2$ in the Cpc-PH and No PH phenotypes than in the other phenotypes (Table 3; Cpc-PH: slope = 0.33, $r = 0.37$, 95% CI [−0.03 to 0.78] and No PH: slope = 0.45, $r = 0.38$, 95% CI [−0.02 to 0.79] vs. $r = -0.09$, 95% CI [−0.41 to 0.22] and $r = -0.13$, 95% CI [−0.29 to 0.03] for precapillary PH and Ipc-PH, respectively).

WIA Components Correlate Differently with RV Function and Hemodynamic Metrics

Given the interpretation of FCWs as RV force generation during early systole, and similar interpretation of end-systolic elastance (E_{es}) as RV contractility (9, 27), we examined the correlation between these two metrics. In both the precapillary PH and No PH phenotypes, FCWs had a significant and moderate positive correlation with E_{es} (Table 3; precapillary PH: $r = 0.45$, 95% CI [0.07–0.82], $P = 0.02$; No PH: $r = 0.57$, 95% CI [0.03–1.11], $P = 0.04$). FCWs and E_{es} were not correlated in Cpc-PH or Ipc-PH.

Next, we assessed BCWs and their relationship with proximal artery stiffness. In Cpc-PH, BCWs were significantly, positively correlated with characteristic impedance (Z_C) (Table 3; $r = 0.64$, 95% CI [0.32–0.96], $P = 0.002$), but no correlations were significant in other phenotypes. In both the combined cohort and precapillary PH, BCWs and pulmonary arterial compliance [PAC, (PAC = stroke volume/pulmonary pulse pressure)] were significantly inversely correlated (Table 3; combined cohort: $r = -0.31$, 95% CI [−0.53 to 0.1], $P = 0.004$; precapillary PH: $r = -0.62$, 95% CI [−1.01 to 0.24], $P = 0.003$). Although BCWs and PAC were not significantly correlated in other phenotypes, all had an inverse relationship. Since the effective arterial elastance (E_a) is also sensitive to proximal artery stiffness (28), we assessed the correlation between BCWs and E_a; a moderate positive correlation was observed between BCWs and E_a only in the precapillary PH phenotype (Table 3; $r = 0.53$, 95% CI [0.13–0.94], $P = 0.01$).

Since FDWs have been interpreted as related to ventricular relaxation in the systemic and coronary circulations (14, 16, 20), we investigated correlations between FDWs and τ. A strong negative correlation was found only in the Cpc-PH phenotype (Table 3; $r = -1.17$, 95% CI [−2.11 to 0.23], $P = 0.03$). We explored relationships between BDWs and metrics of pulmonary vascular properties: PAC (PA compliance) and alpha distensibility (small arteriolar distension). BDWs were significantly inversely correlated with PAC in both the Cpc-PH and No PH phenotypes (Table 3; Cpc-PH: $r = -0.50$, 95% CI [−0.83 to 0.18], $P = 0.006$; No PH: $r = -0.17$, 95% CI [−0.34 to 0.0], $P = 0.045$). No significant correlations were observed between BDWs and distensibility α in any of the phenotypes or in the combined cohort (Table 3). That said, in Cpc-PH and No PH, BDWs had negative correlations with distensibility α ($r = -0.44$, 95% CI[−1.69 to 0.81] and $r = -0.16$, 95% CI [−3.16 to 2.84], respectively). A summary of key significant correlations across PH phenotypes is provided in Table 4.

DISCUSSION

Our study is the first to use wave intensity analysis (WIA) with exercise to identify impairments in RV and pulmonary vascular function across different PH phenotypes. In the combined PH cohort and among four PH phenotypes (pre-capillary PH, Ipc-PH, Cpc-PH, and No PH), our study characterized common and distinct patterns of wave travel, which were phenotype-dependent as well as provocation-dependent (rest-to-exercise). Our main findings, organized by the four components of wave travel (as in Fig. 1), are: *1*) Forward compression waves (FCWs): Cpc-PH participants exhibited the highest FCWs, reflecting highest need for energy expenditure

Table 3. *Linear mixed effects modeling approach comparing WIA components with related RV function and hemodynamic metrics*

Comparison	PH Phenotype	Correlation Coefficient (*r*)	95% Confidence Interval (CI)	*P* Value
FCWs vs. $\dot{V}O_2$*	*Combined*	*0.16*	[*0.02* to *0.31*]	***0.02***
	Precapillary PH	0.18	[−0.08 to 0.43]	0.16
	Ipc-PH	0.17	[−0.02 to 0.35]	0.08
	Cpc-PH	0.10	[−0.61 to 0.81]	0.77
	No PH	0.39	[−0.17 to 0.96]	0.15
BCWs vs. $\dot{V}O_2$*	*Combined*	*0.13*	[*−0.02* to *0.28*]	*0.09*
	Precapillary PH	0.17	[−0.15 to 0.49]	0.28
	Ipc-PH	0.05	[−0.13 to 0.24]	0.58
	Cpc-PH	0.12	[−0.54 to 0.79]	0.68
	No PH	0.92	[0.72 to 0.98]	**<0.0001**
FDWs vs. $\dot{V}O_2$*	*Combined*	*0.20*	[*0.05* to *0.34*]	***0.008***
	Precapillary PH	0.03	[−0.32 to 0.39]	0.85
	Ipc-PH	0.25	[0.07 to 0.43]	**0.008**
	Cpc-PH	0.27	[−0.23 to 0.78]	0.26
	No PH	0.29	[−0.32 to 0.91]	0.30
BDWs vs. $\dot{V}O_2$*	*Combined*	*0.02*	[*−0.11* to *0.15*]	*0.71*
	Precapillary PH	−0.09	[−0.41 to 0.22]	0.54
	Ipc-PH	−0.13	[−0.29 to 0.03]	0.11
	Cpc-PH	0.37	[−0.03 to 0.78]	0.06
	No PH	0.38	[−0.02 to 0.79]	0.06
FCWs vs. E_{es}*	*Combined*	*0.11*	[*−0.11* to *0.33*]	*0.31*
	Precapillary PH	0.45	[0.07 to 0.82]	**0.02**
	Ipc-PH	−0.14	[−0.46 to 0.19]	0.40
	Cpc-PH	0.30	[−0.51 to 1.11]	0.42
	No PH	0.57	[0.03 to 1.11]	**0.04**
BCWs vs. Z_C*	*Combined*	*0.19*	[*−0.01* to *0.39*]	*0.06*
	Precapillary PH	0.22	[−0.4 to 0.84]	0.46
	Ipc-PH	0.07	[−0.22 to 0.35]	0.64
	Cpc-PH	0.64	[0.32 to 0.96]	**0.002**
	No PH	0.41	[−0.06 to 0.89]	0.08
BCWs vs. PAC*	*Combined*	*−0.31*	[*−0.53* to *−0.1*]	***0.004***
	Precapillary PH	−0.62	[−1.01 to −0.24]	**0.003**
	Ipc-PH	−0.15	[−0.48 to 0.17]	0.35
	Cpc-PH	−0.48	[−1.15 to 0.19]	0.14
	No PH	−0.43	[−1.03 to −0.17]	0.14
BCWs vs. E_a*	*Combined*	*0.07*	[*−0.13* to *0.28*]	*0.49*
	Precapillary PH	0.53	[0.13 to 0.94]	**0.01**
	Ipc-PH	0.02	[−0.28 to 0.32]	0.89
	Cpc-PH	0.25	[−0.63 to 1.12]	0.54
	No PH	−0.23	[−0.7 to 0.23]	0.28
FDWs vs. Tau§	*Combined*	*0.07*	[*−0.2* to *0.34*]	*0.59*
	Precapillary PH	−0.15	[−0.66 to 0.37]	0.55
	Ipc-PH	0.25	[−0.11 to 0.6]	0.16
	Cpc-PH	−1.17	[−2.11 to −0.23]	**0.03**
	No PH	−0.63	[−1.79 to 0.53]	0.22
FDWs vs. PAC*	*Combined*	*−0.23*	[*−0.45* to *−0.01*]	***0.04***
	Precapillary PH	−0.17	[−0.63 to 0.29]	0.44
	Ipc-PH	−0.26	[−0.59 to 0.07]	0.12
	Cpc-PH	−0.15	[−0.89 to 0.59]	0.67
	No PH	−0.22	[−0.92 to 0.49]	0.50
FDWs vs. α†	*Combined*	*0.19*	[*−0.21* to *0.59*]	*0.35*
	Precapillary PH	0.39	[−0.89 to 1.67]	0.44
	Ipc-PH	0.12	[−0.50 to 0.75]	0.67
	Cpc-PH	0.17	[−1.20 to 1.54]	0.75
	No PH	0.14	[−2.88 to 3.15]	0.86
BDWs vs. α†	*Combined*	*0.13*	[*−0.31* to *0.56*]	*0.55*
	Precapillary PH	0.27	[−1.07 to 1.60]	0.61
	Ipc-PH	0.36	[−0.33 to 1.04]	0.27
	Cpc-PH	−0.44	[−1.69 to 0.81]	0.38
	No PH	−0.16	[−3.16 to 2.84]	0.84
BDWs vs. PAC*	*Combined*	*−0.08*	[*−0.29* to *0.13*]	*0.46*
	Precapillary PH	0.08	[−0.40 to 0.56]	0.72
	Ipc-PH	0.02	[−0.31 to 0.34]	0.91
	Cpc-PH	−0.50	[−0.83 to −0.18]	**0.006**
	No PH	−0.17	[−0.34 to 0.0]	**0.045**

Continued

Table 3.— *Continued*

Comparison	PH Phenotype	Correlation Coefficient (*r*)	95% Confidence Interval (CI)	*P* Value
BCWs vs. PVR*	*Combined*	*0.13*	[*−0.07* to *0.34*]	*0.21*
	Precapillary PH	0.25	[−0.23 to 0.73]	0.29
	Ipc-PH	0.19	[−0.09 to 0.48]	0.18
	Cpc-PH	0.25	[−0.45 to 0.95]	0.45
	No PH	−0.34	[−1.0 to 0.31]	0.26
Wave Speed vs. Z_C*	*Combined*	*0.20*	[*0.0* to *0.4*]	***0.047***
	Precapillary PH	0.11	[−0.55 to 0.77]	0.73
	Ipc-PH	0.18	[−0.09 to 0.45]	0.18
	Cpc-PH	0.01	[−0.55 to 0.58]	0.96
	No PH	0.37	[−0.29 to 1.03]	0.23
BCWs:FCWs vs. E_{es}/E_a*	*Combined*	*−0.10*	[*−0.31* to *0.12*]	*0.36*
	Precapillary PH	−0.23	[−0.63 to 0.17]	0.24
	Ipc-PH	0.07	[−0.21 to 0.36]	0.61
	Cpc-PH	−0.37	[−0.97 to 0.23]	0.20
	No PH	−0.08	[−0.71 to 0.55]	0.77
BDWs:FDWs vs. DPG*	*Combined*	*−0.09*	[*−0.32* to *0.15*]	*0.46*
	Precapillary PH	0.33	[−0.04 to 0.7]	0.07
	Ipc-PH	−0.11	[−0.44 to 0.22]	0.52
	Cpc-PH	−0.21	[−0.82 to 0.41]	0.46
	No PH	−0.12	[−1.1 to 0.85]	0.78
BDWs:FDWs vs. PVR*	*Combined*	*0.19*	[*−0.02* to *0.4*]	*0.07*
	Precapillary PH	0.10	[−0.38 to 0.58]	0.67
	Ipc-PH	0.17	[−0.13 to 0.46]	0.26
	Cpc-PH	0.29	[−0.29 to 0.87]	0.29
	No PH	0.35	[−0.34 to 1.03]	0.28
BDWs:FDWs vs. PAWP*	*Combined*	*0.00*	[*−0.23* to *0.22*]	*0.99*
	Precapillary PH	−0.36	[−0.87 to 0.16]	0.17
	Ipc-PH	0.10	[−0.25 to 0.44]	0.58
	Cpc-PH	0.23	[−0.38 to 0.85]	0.42
	No PH	−0.17	[−0.70 to 0.36]	0.48

α, alpha distensibility; c, wave speed; BCWs, backward compression waves; BDWs, backward decompression waves; Cpc-PH, combined pre and postcapillary pulmonary hypertension; CRI, compression reflection index; DPG, diastolic pressure gradient; DRI, decompression reflection index; E_a, effective arterial elastance; E_{es}, end systolic elastance; Ees/Ea, RV:PA coupling; FCWs, forward compression waves; FDWs, forward decompression waves; Ipc-PH, isolated post-capillary pulmonary hypertension; PAWP, pulmonary arterial wedge pressure; PAC, pulmonary arterial compliance; PH, pulmonary hypertension; PVR, pulmonary vascular resistance; Tau, right ventricular relaxation time constant; $\dot{V}O_2$, oxygen consumption; Z_C, characteristic impedance. Bold values indicate $P < 0.05$. Italic values indicate 'Combined' group's significant *P*-value. *Total Datapoints: combined $n = 105$, Precapillary PH $n = 23$, Ipc-PH $n = 55$, Cpc-PH $n = 15$, No PH $n = 12$. †Total datapoints for correlations with α: combined $n = 24$, precapillary PH $n = 5$, Ipc-PH $n = 11$, Cpc-PH $n = 5$, No PH $n = 3$. §Total datapoints for correlations with Tau: combined $n = 76$, precapillary PH $n = 23$, Ipc-PH $n = 39$, Cpc-PH $n = 6$, No PH $n = 8$.

by the RV; *2*) Backward compression waves (BCWs): Cpc-PH participants exhibited the highest BCWs, suggesting the greatest proximal pulmonary artery stiffness; *3*) Forward decompression waves (FDWs): pre-capillary PH participants exhibited the highest FDWs, potentially suggesting better RV relaxation during early diastole; and *4*) Backward decompression waves (BDWs): precapillary PH participants exhibited the highest BDWs during exercise, correlating with increased pulmonary arterial stiffness (decreased compliance) in Cpc-PH. In addition, we report that *5*) the compression wave reflection index (BCWs:FCWs) decreased in Ipc-PH during exercise, suggesting RV reserve capacity that improves vascular-ventricular coupling. Overall, our results demonstrate that wave intensity analysis of pulmonary vascular hemodynamics at rest and exercise reveals ventricle and vessel-specific impairments that are distinct in different PH phenotypes, underscoring both the complexity of cardiopulmonary wave travel and the need for further research to improve phenotype-specific interventions.

RV Contraction (Forward Compression Waves)

Consistent with an RV ejecting against high afterload, the Cpc-PH phenotype had the highest FCWs at rest and during initial exercise (25 W). This finding is in agreement with the recent work of Yim et al. (11), who found that in patients with PH due to left heart disease, FCW intensity correlated with RV stroke work index and mPAP. At 100 W, the precapillary PH phenotype had nearly twice the FCWs as the Ipc-PH phenotype, which is also consistent with prior findings of greater RV contractility in precapillary PH compared with Ipc-PH (29, 30). This link between FCWs and RV contractility in precapillary PH is further supported by our findings in Table 3, where a significant positive correlation between FCWs and E_{es} ($P = 0.02$) was observed. In contrast, no such correlation was found in either of the PH-HFpEF phenotypes (i.e., Ipc-PH and Cpc-PH), likely due to complex mechanisms underlying RV dysfunction in left heart disease (e.g., added component of intrinsic myocardial disease and interventricular interactions) (31, 32).

Proximal PA Stiffness (Backward Compression Waves)

BCWs provide insights into proximal pulmonary artery stiffness, which is a key contributor to RV afterload. At rest and during exercise, Cpc-PH exhibited the highest BCWs, evidencing greatest pulmonary artery reflections. Precapillary PH had higher BCWs than Ipc-PH and No PH, which parallels the previously reported greater rest-to-exercise effective arterial elastance (E_a) in precapillary PH compared with Ipc-PH and No PH (33) [Lechuga et al. (33); a Cpc-PH phenotype was not included in the study]. As expected in precapillary PH,

Table 4. *Summary of statistically significant WIA correlations across PH phenotypes*

PH Phenotype	Key Correlations	Interpretation Summary
Precapillary PH	↑ FCWs ∼ ↑ E_{es} ($r = 0.45$, $P = 0.02$) ↑ BCWs ∼ ↑ E_a ($r = 0.53$, $P = 0.01$) ↑ BCWs ∼ ↓ PAC ($r = -0.62$, $P = 0.003$)	Strong RV contraction and increased proximal PA stiffness in response to increased afterload and decreased compliance.
Ipc-PH	↑ FDWs ∼ ↑ $\dot{V}O_2$ ($r = 0.25$, $P = 0.008$)	Preserved diastolic relaxation contributes to maintained exercise capacity.
Cpc-PH	↑ BCWs ∼ ↑ Z_C ($r = 0.64$, $P = 0.002$) ↑ BDWs ∼ ↓ PAC ($r = -0.50$, $P = 0.006$) ↑ FDWs ∼ ↓ τ ($r = -1.17$, $P = 0.03$)	Increased proximal PA and distal pulmonary vascular stiffness; abnormal RV relaxation.
No PH	↑ FCWs ∼ ↑ E_{es} ($r = 0.57$, $P = 0.04$) ↑ BDWs ∼ ↓ PAC ($r = -0.17$, $P = 0.045$) ↑ BCWs ∼ ↑ $\dot{V}O_2$ ($r = 0.92$, $P < 0.0001$)	Strong RV contraction and high pulmonary compliance needed for good $\dot{V}O_2$ response.

BCWs, backward compression waves; BDWs, backward decompression waves; Cpc-PH, combined pre and postcapillary pulmonary hypertension; E_a, effective arterial elastance; E_{es}, end systolic elastance; FCWs, forward compression waves; FDWs, forward decompression waves; Ipc-PH, isolated post-capillary pulmonary hypertension; PAC, pulmonary arterial compliance; PH, pulmonary hypertension; Tau (τ), right ventricular relaxation time constant; $\dot{V}O_2$, oxygen consumption; Z_C, characteristic impedance. This table highlights the key significant correlations observed between WIA components (FCWs, BCWs, FDWs, BDWs) and hemodynamic metrics (e.g., E_{es}, E_a, PAC, Z_C, $\dot{V}O_2$) across four PH phenotypes. The physiological interpretation provides a brief contextual understanding of how these relationships reflect underlying vascular and ventricular mechanics in each phenotype. ↑ Indicates 'increasing' value of reported metric, ↓ indicates 'decreasing value' of reported metric.

BCWs were negatively correlated with PAC (compliance, $P = 0.003$) and positively correlated with E_a ($P = 0.01$) in our study. For PH due to left heart disease (Ipc-PH, Cpc-PH), Yim et al. (11) reported that participants with BCWs had significantly decreased PAC and increased mPAP, compared with participants without BCWs (albeit they did not compute E_a or Z_C). We report that in Cpc-PH, BCWs significantly correlated with characteristic impedance (Z_C, $P = 0.002$) (Table 3). These observations suggest that while BCWs contribute to RV afterload, they reflect distinct aspects of pathobiology among PH phenotypes (E_a and the inverse of PAC in precapillary PH vs. Z_C in Cpc-PH).

The compression reflection index (BCWs:FCWs) parallels metrics of vascular-ventricular coupling (i.e., the inverse of ventricular-vascular coupling E_{es}/E_a), since BCWs relate to RV afterload, whereas FCWs reflect RV force generation (14). At rest, the compression reflection index was similar across the PH phenotypes (∼30%) and higher than that in the No PH phenotype (∼9%), though these differences were not significant (Fig. 4). Su et al. (13) similarly found PAH and CTEPH participants had comparable wave reflection indices at rest (∼28%), which were significantly greater indices than control participants (∼4%) (34). We previously found higher E_{es}/E_a in No PH and PH-HFpEF participants than precapillary PH (33), which is also consistent with these findings (9). However, during exercise, BCWs:FCWs decreased in Ipc-PH, did not change in Cpc-PH or precapillary PH, and tended to increase in No PH (Fig. 4). This result suggests that in Ipc-PH, RV force generation overcomes RV afterload to accommodate increased blood flow demands. In contrast, in Cpc-PH and precapillary PH, the RV is less able to increase force generation to meet the rising demand during exercise. Overall, the compression reflection index (BCWs:FCWs) provides a measure of vascular-ventricular coupling that is sensitive to PH phenotype as well as changes in RV afterload with exercise.

RV Relaxation (Forward Decompression Waves)

Beyond the relatively clear physiological implications of the compression waves that typically occur in systole, the decompression waves FDW and BDW, which typically occur during diastole, are less understood or studied in the pulmonary circulation. Based on clinical and computational studies, FDWs are interpreted as measures of ventricular relaxation and RV outflow deceleration (15, 16, 20, 35, 36). The consistently higher FDWs in precapillary PH compared with the other PH phenotypes, both at rest and during exercise (Fig. 2*C*), may suggest more intact RV relaxation in this cohort, but further investigation is required to confirm this interpretation. We investigated the correlation between FDWs and the RV relaxation factor τ for each PH phenotype and found a significantly strong negative relationship in the Cpc-PH phenotype (Table 3, $r = -1.17$, $P = 0.03$). Given that Cpc-PH is not typically associated with enhanced diastolic function, this finding appears counterintuitive, raising the possibility that FDWs may have a different physiological role in the pulmonary circulation than in the coronary circulation. We speculate that in Cpc-PH, where diastolic dysfunction is often present, FDWs may instead be driven by altered pressure gradients or abnormal wave reflection timing rather than efficient myocardial relaxation. One possible mechanism is delayed pulmonary valve closure or recoil from stiffer upstream vessels producing a false signal of relaxation. Alternatively, compliance mismatch between stiff proximal arteries and less compliant distal vessels may distort wave propagation, altering FDWs due to distal vascular segments impeding forward blood flow independent of true diastolic function. Further research is needed to clarify the mechanisms underlying FDWs and their implications for RV-pulmonary vascular interactions.

Distal Pulmonary Vascular Stiffness (Backward Decompression Waves)

BDWs are related to wave travel in an antegrade direction during diastole; in the coronary circulation they are interpreted as a measure of distal vascular properties, including compliance and elastic recoil (17, 37, 38). Their physiological meaning in the pulmonary circulation remains unclear. We speculate that BDWs reflect diastolic flow acceleration produced by proximal vascular recoil and shaped by the distribution and magnitude of downstream resistance. This differs from the coronary

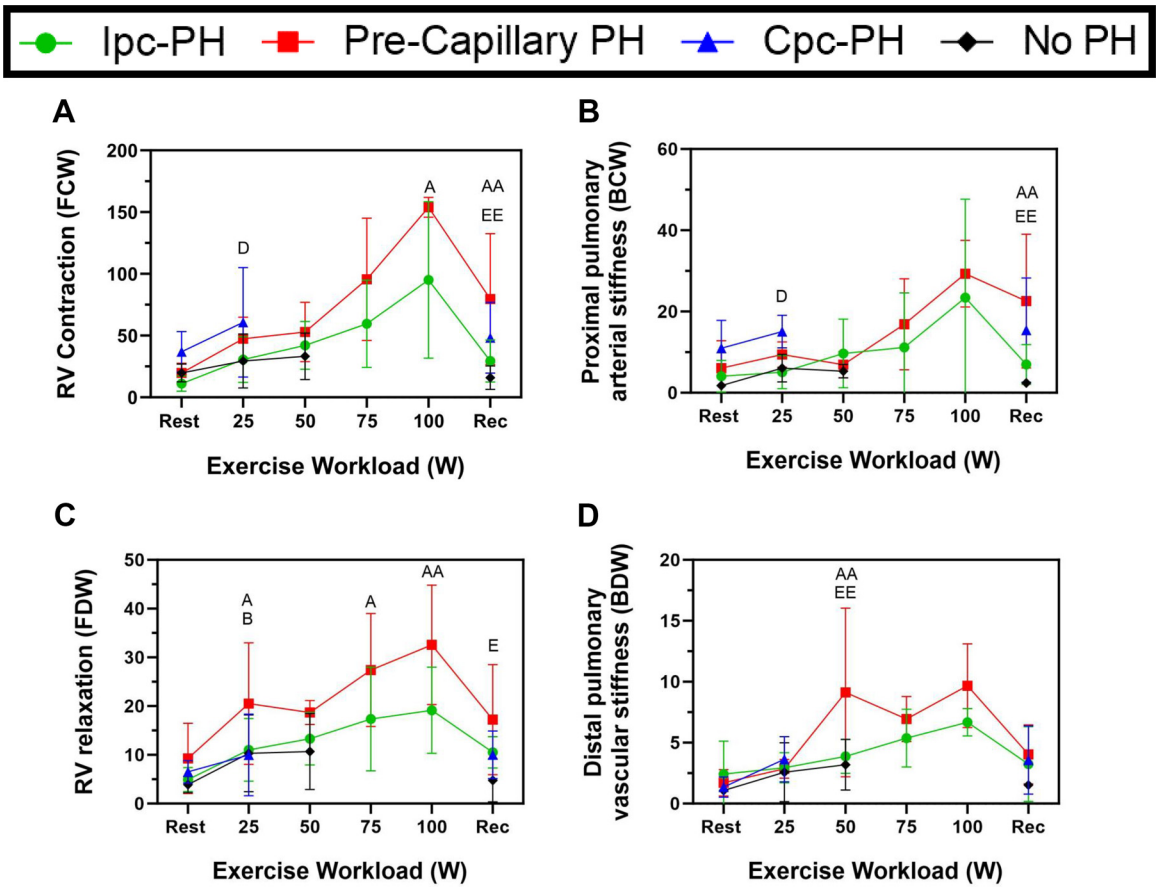

Figure 2. Wave intensity analysis (WIA) in pulmonary hypertension phenotypes during exercise. Group average: forward compression waves (FCWs) (*A*), backward compression waves (BCWs) (*B*), forward decompression waves (FDWs) (*C*), and backward decompression waves (BDWs) (*D*) for Ipc-PH ($n = 12$), precapillary PH ($n = 5$), Cpc-PH ($n = 5$), and No PH ($n = 3$) at rest, during exercise, and at recovery. $^{A}P < 0.05$, $^{AA}P < 0.01$ for intergroup comparisons between precapillary PH vs. Ipc-PH phenotypes. $^{B}P < 0.05$, $P < 0.01$ for intergroup comparisons between Cpc-PH vs. precapillary PH. $P < 0.05$, $P < 0.01$ for intergroup comparisons between Ipc-PH vs. No PH. $^{D}P < 0.05$, $P < 0.01$ for intergroup comparisons between Cpc-PH vs. Ipc-PH. $^{E}P < 0.05$, $^{EE}P < 0.01$ for intergroup comparisons between precapillary PH vs. No PH. $P < 0.05$, $P < 0.01$ for intergroup comparisons between Cpc-PH vs. No PH. Cpc-PH, combined pre and postcapillary pulmonary hypertension; Ipc-PH, isolated postcapillary pulmonary hypertension.

circulation, where BDWs are tightly coupled to myocardial relaxation and reperfusion of the sub-endocardium. In precapillary PH, increased wave speed suggests proximal arterial stiffening, which may enhance elastic recoil during diastole. Because resistance is concentrated at the arteriolar level and the venous system remains relatively compliant, diastolic flow can accelerate more readily, resulting in larger BDWs. In Cpc-PH, however, elevated left atrial pressure and postcapillary remodeling (venular remodeling) introduce significant distal resistance, blunting the ability of recoil forces to accelerate blood flow during diastole and leading to smaller BDWs despite similarly elevated proximal stiffness. Ipc-PH may show relatively higher BDWs at rest due to the equal distribution of resistance in the arteriolar, capillary, and venous systems. This distribution may create a more permissive environment for diastolic flow acceleration during rest, even in the presence of elevated wedge pressures. These insights suggest that BDWs can serve as a potential indicator of the distal resistance profile and the capacity for diastolic flow accommodation in different forms of PH. Our findings reveal significant, negative correlations between BDWs and PAC in both the Cpc-PH and No PH phenotypes and non-significant negative correlations with distensibility α ($r = -0.44$ and $r = -0.16$, respectively). The lack of significant correlations in precapillary PH and Ipc-PH reinforces the need for further investigation to better understand the physiological interpretation of BDWs in the pulmonary circulation.

Clinical Relevance

The physiological and clinical relevance of WIA components is emphasized by their relationship with oxygen consumption: $\dot{V}O_2$ from rest to exercise. Notably, maximum achievable workload differed markedly across phenotypes in our cohort: Cpc-PH participants reached a mean of 28 W, whereas precapillary PH, Ipc-PH, and No PH groups achieved higher workloads on average (67 W, 76 W, and 72 W, respectively). These findings align with the pathophysiological severity of Cpc-PH, which involves both pre- and postcapillary components (39, 40), and support the notion that symptom burden and exercise intolerance vary inherently across PH groups. This inherent variability likely contributes to the differential patterns observed in wave intensity and their correlations with $\dot{V}O_2$.

Moreover, although in this study with exercise testing, by design, we included PH participants with mild-moderate PH, we anticipate that some unique WIA patterns would

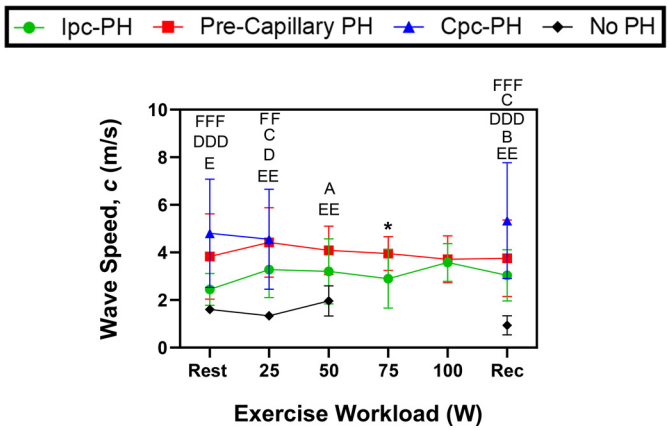

Figure 3. Wave speed in pulmonary hypertension phenotypes during exercise. Group average pulmonary arterial wave speed for Ipc-PH ($n = 12$), precapillary PH ($n = 5$), Cpc-PH ($n = 5$), and No PH ($n = 3$) at rest, during exercise, and at recovery. $^{A}P < 0.05$, $P < 0.01$, $P < 0.001$ for intergroup comparisons between precapillary PH vs. Ipc-PH phenotypes. $^{B}P < 0.05$, $P < 0.01$, $P < 0.001$ for intergroup comparisons between Cpc-PH vs. precapillary PH phenotypes. $^{C}P < 0.05$, $P < 0.01$, $P < 0.001$ for intergroup comparisons between Ipc-PH vs. No PH phenotypes. $^{D}P < 0.05$, $P < 0.01$, $^{DDD}P < 0.001$ for intergroup comparisons between Cpc-PH vs. Ipc-PH phenotypes. $^{E}P < 0.05$, $^{EE}P < 0.01$, $P < 0.001$ for intergroup comparisons between precapillary PH vs. No PH phenotypes. $P < 0.05$, $^{FF}P < 0.01$, $^{FFF}P < 0.001$ for intergroup comparisons between Cpc-PH vs. No PH phenotypes. Cpc-PH, combined pre- and postcapillary pulmonary hypertension; Ipc-PH, isolated postcapillary pulmonary hypertension.

arise in patients with severe PH in whom exercise testing is not possible. In particular, we anticipate that as PH worsens, BCW intensity would increase with PA stiffness and FCW would decrease with decreased RV stroke volume. We would also expect decreased intensity of FDW (poor RV relaxation) and increased BDW (distal pulmonary vascular stiffness), albeit with less confidence given the less obvious rest behaviors of decompression waves.

Based on correlation coefficients, the stronger positive correlation between FCWs and $\dot{V}O_2$ in the No PH phenotype

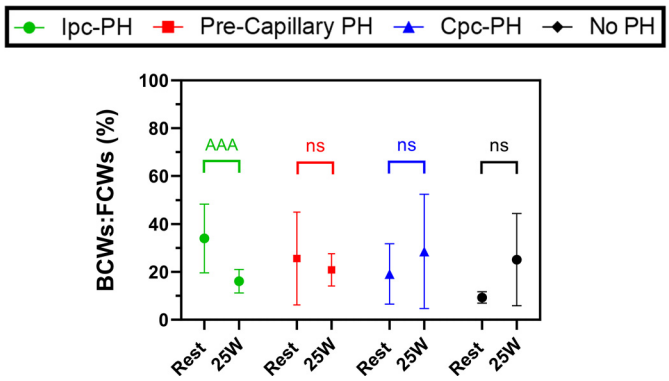

Figure 4. Compression reflection indices in pulmonary hypertension phenotypes during exercise. Group average compression reflection indices calculated as the ratio of backward compression waves (BCWs) to forward compression waves (FCWs) at rest and during initial exercise for Ipc-PH ($n = 12$), precapillary PH ($n = 5$), Cpc-PH ($n = 5$), and No PH ($n = 3$) at rest, during exercise, and at recovery. $P < 0.05$, $P < 0.01$, $^{AAA}P < 0.001$ for intragroup comparisons between rest and initial exercise for each phenotype. Cpc-PH, combined pre- and postcapillary pulmonary hypertension; Ipc-PH, isolated postcapillary pulmonary hypertension.

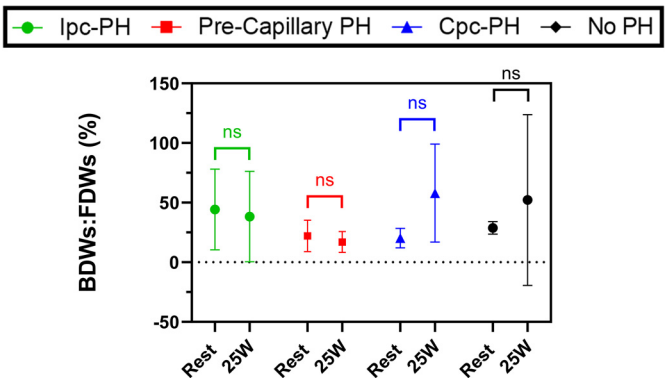

Figure 5. Decompression reflection indices in pulmonary hypertension phenotypes during exercise. Group average decompression reflection indices calculated as the ratio of backward decompression waves (BDWs) to forward decompression waves (FDWs) at rest and during initial exercise for Ipc-PH ($n = 12$), precapillary PH ($n = 5$), Cpc-PH ($n = 5$), and No PH ($n = 3$) at rest, during exercise, and at recovery. $P < 0.05$, $P < 0.01$, $P < 0.001$ for intragroup comparisons between rest and initial exercise for each phenotype. Cpc-PH, combined pre- and postcapillary pulmonary hypertension; Ipc-PH, isolated postcapillary pulmonary hypertension.

suggests that RV contractility is more closely linked to aerobic capacity in non-diseased participants (Table 3, Supplemental Fig. S1; see https://doi.org/10.5281/zenodo.16500282). Similarly, the correlation between BCWs and $\dot{V}O_2$ is even stronger in the No PH phenotype ($P < 0.0001$, slope $= +0.92$); however, this does not imply that higher BCWs enhance functional capacity in this group. Rather, No PH participants exhibited greater $\dot{V}O_2$ increases despite relatively smaller BCW changes, whereas PH groups maintained higher BCWs with minimal $\dot{V}O_2$ gains, leading to the observed correlation differences. Altogether, the physiological significance of BCWs in relation to exercise capacity remains unclear and may differ between healthy and diseased states, warranting further investigation. The absence of a similar relationship in PH phenotypes may suggest that pulmonary vascular disease disrupts the RV's ability to manage reflected waves, contributing to exercise intolerance. These findings highlight the significance of wave reflections and RV-pulmonary interactions in influencing exercise capacity but also emphasize the need for further research to clarify their specific role in different cardiopulmonary conditions.

Study Limitations and Summary

The major limitation of this study is the small sample size, which is common to prospective invasive, multimodal exercise studies, especially in PH. Another limitation is variability in maximum workload across participants, which is also common to exercise PH studies. Since all participants achieved initial exercise (25 W), we focused on wave reflection index on this workload, and for the rest of the metrics our statistical analyses accounted for the exercise workload each participant achieved. The variability in WIA metrics with exercise within precapillary PH is especially evident (Fig. 2), which may be related to the combination of two WHO PH groups (PAH and CTEPH) within this group (Table 1). Future studies will be needed to discriminate WIA patterns in PAH and CTEPH. In addition, the current study is based on a single rest-to-exercise test in each subject. Given day-to-day and subject-to-subject variability,

repeated testing under different loading conditions or after treatment would allow more robust comparisons between cohorts with potential normalization to subject-specific WIA metrics at rest.

In summary, our study demonstrates the utility of WIA in revealing distinct ventricle- and vessel-specific differences in PH phenotypes. WIA metrics, including FCWs, BCWs, FDWs, and BDWs, offer insight into RV force generation, pulmonary artery stiffness, RV relaxation, and distal pulmonary vascular mechanics. In addition, the compression reflection index provides a complementary metric of pulmonary artery-RV coupling. Future studies with larger cohorts and additional provocations, such as vasoreactivity testing, will be critical in assessing the broader diagnostic potential of WIA and its sensitivity to treatment efficacy.

DATA AVAILABILITY

Materials used, data gathered, and methods applied in this research will be made available upon reasonable request in writing for purposes of reproduction and/or replication.

SUPPLEMENTAL MATERIAL

Supplemental Fig. S1: https://doi.org/10.5281/zenodo.16500282.

GRANTS

This study was supported by the National Center for Advancing Translational Sciences, Grant/Award No.: KL2TR002374-07 (to F.R.), American Heart Association, Grant/Award No.: 23CDA1057697 (to F.R.), the NIH T32HL116270 (to C.G.L.), NIH R01HL154624 (to N.C.C.), and NIH R01HL147590 (to N.C.C.). M.J.C. was supported by the National Center for Research Resources and the National Center for Advancing Translational Sciences, National Institutes of Health, through Grant TL1001415.

DISCLAIMERS

The content is solely the responsibility of the authors and does not necessarily represent the official views of the NIH.

DISCLOSURES

No conflicts of interest, financial or otherwise, are declared by the authors.

AUTHOR CONTRIBUTIONS

C.G.L., F.R., and N.C.C. conceived and designed research; C.G.L., F.R., and C.E.K. performed experiments; C.G.L., M.J.C., C.E.K., and J.C.E. analyzed data; C.G.L., F.R., M.J.C., J.C.E., and N.C.C. interpreted results of experiments; C.G.L. prepared figures; C.G.L. drafted manuscript; C.G.L., F.R., M.J.C., and N.C.C. edited and revised manuscript; C.G.L., F.R., M.J.C., C.E.K., J.C.E., and N.C.C. approved final version of manuscript.

REFERENCES

1. **Rajagopal S**, **Ruetzler K**, **Ghadimi K**, **Horn EM**, **Kelava M**, **Kudelko KT**, **Moreno-Duarte I**, **Preston I**, **Rose Bovino LL**, **Smilowitz NR**, **Vaidya A**; **American Heart Association Council on Cardiopulmonary, Critical Care, Perioperative and Resuscitation, and the Council on Cardiovascular and Stroke Nursing.** Evaluation and management of pulmonary hypertension in noncardiac surgery: a scientific statement from the American Heart Association. *Circulation* 147: 1317–1343, 2023. doi:10.1161/CIR.0000000000001136.
2. **Bousseau S**, **Sobrano Fais R**, **Gu S**, **Frump A**, **Lahm T.** Pathophysiology and new advances in pulmonary hypertension. *BMJ Med* 2: e000137, 2023. doi:10.1136/bmjmed-2022-000137.
3. **Chang KY**, **Duval S**, **Badesch DB**, **Bull TM**, **Chakinala MM**, **De Marco T**, **Frantz RP**, **Hemnes A**, **Mathai SC**, **Rosenzweig EB**, **Ryan JJ**, **Thenappan T**; **PHAR Investigators.** Mortality in pulmonary arterial hypertension in the modern era: early insights from the pulmonary hypertension association registry. *J Am Heart Assoc* 11: e024969, 2022. doi:10.1161/JAHA.121.024969.
4. **Novoyatleva T.** Pulmonary hypertension: new insights and recent advances from basic science to translational approaches. *Int J Mol Sci* 24: 8462, 2023. doi:10.3390/ijms24108462.
5. **Maron BA**, **Kovacs G**, **Vaidya A**, **Bhatt DL**, **Nishimura RA**, **Mak S**, **Guazzi M**, **Tedford RJ.** Cardiopulmonary hemodynamics in pulmonary hypertension and heart failure: JACC review topic of the week. *J Am Coll Cardiol* 76: 2671–2681, 2020. doi:10.1016/j.jacc.2020.10.007.
6. **Assad TR**, **Hemnes AR**, **Larkin EK**, **Glazer AM**, **Xu M**, **Wells QS**, **Farber-Eger EH**, **Sheng Q**, **Shyr Y**, **Harrell FE**, **Newman JH**, **Brittain EL.** Clinical and biological insights into combined post-capillary and pre-capillary pulmonary hypertension. *J Am Coll Cardiol* 68: 2525–2536, 2016. doi:10.1016/j.jacc.2016.09.942.
7. **Chesler NC**, **Roldan A**, **Vanderpool RR**, **Naeije R.** How to measure pulmonary vascular and right ventricular function. *31st Annual International Conference of the IEEE Engineering in Medicine and Biology Society (EMBC 2009)*. Minneapoli, MN, Sep 2–6, 2009, p. 772–180.
8. **Sabbahi A**, **Severin R**, **Ozemek C**, **Phillips SA**, **Arena R.** The role of cardiopulmonary exercise testing and training in patients with pulmonary hypertension: making the case for this assessment and intervention to be considered a standard of care. *Expert Rev Respir Med* 14: 317–327, 2020. doi:10.1080/17476348.2020.1708196.
9. **Raza F**, **Kozitza C**, **Lechuga C**, **Seiter D**, **Corrado P**, **Merchant M**, **Dharmavaram N**, **Korcarz C**, **Eldridge M**, **Francois C**, **Wieben O**, **Chesler N.** Multimodality deep phenotyping methods to assess mechanisms of poor right ventricular–pulmonary artery coupling. *Function* 3: zqac022, 2022. doi:10.1093/function/zqac022.
10. **Humbert M**, **Kovacs G**, **Hoeper MM**, **Badagliacca R**, **Berger RMF**, **Brida M**, **Carlsen J**, **Coats AJS**, **Escribano-Subías P**, **Ferrari P**, **Ferreira DS**, **Ghofrani HA**, **Giannakoulas G**, **Kiely DG**, **Mayer E**, **Meszaros G**, **Nagavci B**, **Olsson KM**, **Pepke-Zaba J**, **Quint JK**, **Rådegran G**, **Simonneau G**, **Sitbon O**, **Tonia T**, **Toshner M**, **Vachiery JL**, **Vonk Noordegraaf A**, **Delcroix M**, **Rosenkranz S**; **ESC/ERS Scientific Document Group.** 2022 ESC/ERS guidelines for the diagnosis and treatment of pulmonary hypertension developed by the task force for the diagnosis and treatment of pulmonary hypertension of the European Society of Cardiology (ESC) and the European Respiratory Society (ERS). Endorsed by the International Society for Heart and Lung Transplantation (ISHLT) and the European Reference Network on rare respiratory diseases (ERN-LUNG). *Eur Heart J* 43: 3618–3731, 2022. doi:10.1093/eurheartj/ehac237.
11. **Yim IHW**, **Parker KH**, **Drury NE**, **Lim HS.** Pulmonary artery wave intensity analysis in pulmonary hypertension associated with heart failure and reduced left ventricular ejection fraction. *Pulm Circ* 14: e12345, 2024. doi:10.1002/pul2.12345.
12. **Yim I**, **Parker K**, **Lim S.** Pulmonary artery wave intensity analysis in pulmonary hypertension due to left heart disease. *J Heart Lung Transplant* 41: S139–S140, 2022. doi:10.1016/j.healun.2022.01.327.
13. **Su J**, **Manisty C**, **Parker KH**, **Simonsen U**, **Nielsen-Kudsk JE**, **Mellemkjaer S**, **Connolly S**, **Lim PB**, **Whinnett ZI**, **Malik IS**, **Watson G**, **Davies JE**, **Gibbs S**, **Hughes AD**, **Howard L.** Wave intensity analysis provides novel insights into pulmonary arterial hypertension and chronic thromboembolic pulmonary hypertension. *J Am Heart Assoc* 6: e006679, 2017. doi:10.1161/JAHA.117.006679.
14. **Parker KH.** An introduction to wave intensity analysis. *Med Biol Eng Comput* 47: 175–188, 2009. doi:10.1007/s11517-009-0439-y.
15. **Qureshi MU**, **Hill NA.** A computational model study of pressure wave reflections in the pulmonary arteries. *J Math Biol* 71: 1525–1549, 2015. doi:10.1007/s00285-015-0867-2.
16. **Bouwmeester JC**, **Park J**, **Valdovinos J**, **Bonde P.** Wave intensity analysis of right ventricular function during pulsed operation of rotary left ventricular assist devices. *ASAIO J* 65: 465–472, 2019. doi:10.1097/MAT.0000000000000835.

17. **Broyd CJ**, **Davies JE**, **Escaned JE**, **Hughes A**, **Parker K.** Wave intensity analysis and its application to the coronary circulation. *Glob Cardiol Sci Pract* 2017: e201705, 2017. doi:10.21542/gcsp.2017.5.
18. **Lau EMT**, **Abelson D**, **Dwyer N**, **Yu Y**, **Ng MK**, **Celermajer DS.** Assessment of ventriculo-arterial interaction in pulmonary arterial hypertension using wave intensity analysis. *Eur Respir J* 43: 1804–1807, 2014. doi:10.1183/09031936.00148313.
19. **Quail MA**, **Knight DS**, **Steeden JA**, **Taelman L**, **Moledina S**, **Taylor AM**, **Segers P**, **Coghlan JG**, **Muthurangu V.** Noninvasive pulmonary artery wave intensity analysis in pulmonary hypertension. *Am J Physiol Heart Circ Physiol* 308: H1603–H1611, 2015. doi:10.1152/ajpheart.00480.2014.
20. **Schäfer M**, **Wilson N**, **Ivy DD**, **Ing R**, **Abman S**, **Browne LP**, **Morgan G**, **Ross M**, **McLennan D**, **Barker AJ**, **Fonseca B**, **Di Maria M**, **Hunter KS**, **Truong U.** Noninvasive wave intensity analysis predicts functional worsening in children with pulmonary arterial hypertension. *Am J Physiol Heart Circ Physiol* 315: H968–H977, 2018. doi:10.1152/ajpheart.00227.2018.
21. **Zhong XJ**, **Jiang R**, **Yang L**, **Yuan P**, **Gong SG**, **Zhao QH**, **Luo CJ**, **Qiu HL**, **Li HT**, **Zhang R**, **He J**, **Wang L**, **Tang J**, **Liu JM.** Peak oxygen uptake is a strong prognostic predictor for pulmonary hypertension due to left heart disease. *BMC Cardiovasc Disord* 22: 137–137, 2022. doi:10.1186/s12872-022-02574-0.
22. **Weatherald J**, **Farina S**, **Bruno N**, **Laveneziana P.** Cardiopulmonary exercise testing in pulmonary hypertension. *Ann Am Thorac Soc* 14: S84–S92, 2017. doi:10.1513/AnnalsATS.201610-788FR.
23. **Kozitza CJ**, **Dharmavaram N**, **Tao R**, **Tabima DM**, **Chesler NC**, **Raza F.** Pulmonary vascular distensibility with passive leg raise is comparable to exercise and predictive of clinical outcomes in pulmonary hypertension. *Pulm Circ* 12: e12029, 2022. doi:10.1002/pul2.12029.
24. **Tao R**, **Dharmavaram N**, **El Shaer A**, **Heffernan S**, **Tu W**, **Ma J**, **Garcia-Arango M**, **Baber A**, **Dhingra R**, **Runo J**, **Masri SC**, **Rahko P**, **Raza F.** Relationship of TAPSE normalized by right ventricular area with pulmonary compliance, exercise capacity, and clinical outcomes. *Circ Heart Fail* 17: e010826, 2024. doi:10.1161/CIRCHEARTFAILURE.123.010826.
25. **El Shaer A**, **Garcia-Arango M**, **Korcarz C**, **Broman AT**, **Lechuga CG**, **Chesler NC**, **Raza F.** Right ventricular outflow tract diameter change with exercise: a prospective exercise echocardiography and invasive CPET study. *Eur Heart J Imaging Methods Pract* 2: qyae039, 2024. doi:10.1093/ehjimp/qyae039.
26. **Nichols WW**, **O'Rourke MF**, **Edelman ER**, **Vlachopoulos C.** *Mcdonald's Blood Flow in Arteries: Theoretical, Experimental and Clinical*. CRC Press, 2022.
27. **Richter MJ**, **Peters D**, **Ghofrani HA**, **Naeije R**, **Roller F**, **Sommer N**, **Gall H**, **Grimminger F**, **Seeger W**, **Tello K.** Evaluation and prognostic relevance of right ventricular-arterial coupling in pulmonary hypertension. *Am J Respir Crit Care Med* 201: 116–119, 2020. doi:10.1164/rccm.201906-1195LE.
28. **Brener MI**, **Burkhoff D**, **Sunagawa K.** Effective arterial elastance in the pulmonary arterial circulation: derivation, assumptions, and clinical applications. *Circ Heart Fail* 13: e006591, 2020 [Erratum in *Circ Heart Fail* 13: e000038, 2020]. doi:10.1161/CIRCHEARTFAILURE.119.006591.
29. **Oakland H**, **Joseph P**, **Naeije R**, **Elassal A**, **Cullinan M**, **Heerdt PM**, **Singh I.** Arterial load and right ventricular-vascular coupling in pulmonary hypertension. *J Appl Physiol (1985)* 131: 424–433, 2021. doi:10.1152/japplphysiol.00204.2021.
30. **Singh I**, **Oliveira RKF**, **Naeije R**, **Rahaghi FN**, **Oldham WM**, **Systrom DM**, **Waxman AB.** Pulmonary vascular distensibility and early pulmonary vascular remodeling in pulmonary hypertension. *Chest* 156: 724–732, 2019. doi:10.1016/j.chest.2019.04.111.
31. **Zampierollo-Jaramillo G**, **Abed A**, **El Shaer A**, **Garcia-Arango M**, **Chen Y**, **Tehrani B**, **Tu W**, **Arif AW**, **Heffernan S**, **Esmaeeli A**, **Sahai A**, **Runo J**, **Baber A**, **Masri SC**, **Raza F.** Ventricular interdependent phenotype of mixed Cpc-pulmonary hypertension and HFpEF with normal left atrium: Impact on CPET metrics and clinical outcomes. *Pulm Circ* 14: e12449, 2024. doi:10.1002/pul2.12449.
32. **Patel RB**, **Li E**, **Benefield BC**, **Swat SA**, **Polsinelli VB**, **Carr JC**, **Shah SJ**, **Markl M**, **Collins JD**, **Freed BH.** Diffuse right ventricular fibrosis in heart failure with preserved ejection fraction and pulmonary hypertension. *ESC Heart Fail* 7: 253–263, 2020. doi:10.1002/ehf2.12565.
33. **Lechuga CG**, **Raza F**, **Colebank MJ**, **Korcarz CE**, **Broman AT**, **Eickhoff JC**, **Chesler NC.** Characteristic pulmonary impedance with exercise detects abnormal pulmonary vascular response and uncoupling in pulmonary hypertension resulting from heart failure with preserved ejection fraction. *Chest* 168: 488–501, 2025. doi:10.1016/j.chest.2025.02.019.
34. **Glass A**, **McCall P**, **Arthur A**, **Mangion K**, **Shelley B.** Pulmonary artery wave reflection and right ventricular function after lung resection. *Br J Anaesth* 130: e128–e136, 2023. doi:10.1016/j.bja.2022.07.052.
35. **Parker KH**, **Jones CJ**, **Dawson JR**, **Gibson DG.** What stops the flow of blood from the heart? *Heart Vessels* 4: 241–245, 1988. doi:10.1007/BF02058593.
36. **Jones CJH**, **Sugawara M**, **Kondoh Y**, **Uchida K**, **Parker KH.** Compression and expansion wavefront travel in canine ascending aortic flow: wave intensity analysis. *Heart Vessels* 16: 91–98, 2002. doi:10.1007/s003800200002.
37. **Tyberg JV**, **Davies JE**, **Wang Z**, **Whitelaw WA**, **Flewitt JA**, **Shrive NG**, **Francis DP**, **Hughes AD**, **Parker KH**, **Wang JJ.** Wave intensity analysis and the development of the reservoir-wave approach. *Med Biol Eng Comput* 47: 221–232, 2009. doi:10.1007/s11517-008-0430-z.
38. **Ladwiniec A**, **White PA**, **Nijjer SS**, **O'Sullivan M**, **West NEJ**, **Davies JE**, **Hoole SP.** Diastolic backward-traveling decompression (suction) wave correlates with simultaneously acquired indices of diastolic function and is reduced in left ventricular stunning. *Circ Cardiovasc Interv* 9: e003779, 2016. doi:10.1161/CIRCINTERVENTIONS.116.003779.
39. **Allen BJ**, **Frye H**, **Ramanathan R**, **Caggiano LR**, **Tabima DM**, **Chesler NC**, **Philip JL.** Biomechanical and mechanobiological drivers of the transition from postcapillary pulmonary hypertension to combined pre−/postcapillary pulmonary hypertension. *J Am Heart Assoc* 12: e028121, 2023. doi:10.1161/JAHA.122.028121.
40. **Aradhyula V**, **Vyas R**, **Dube P**, **Haller ST**, **Gupta R**, **Maddipati KR**, **Kennedy DJ**, **Khouri SJ.** Novel insights into the pathobiology of pulmonary hypertension in heart failure with preserved ejection fraction. *Am J Physiol Heart Circ Physiol* 326: H1498–H1514, 2024. doi:10.1152/ajpheart.00068.2024.